Low-Complexity Near-Optimal Detector for Multiple-Input Multiple-Output OFDM with Index Modulation

Beixiong Zheng*, Miaowen Wen*, Ertugrul Basar†, and Fangjiong Chen*
*School of Electronic and Information Engineering, South China University of Technology, Guangzhou 510641, China
†Istanbul Technical University, Faculty of Electrical and Electronics Engineering 34469, Istanbul, Turkey

***Abstract*—Multiple-input multiple-output orthogonal frequency division multiplexing with index modulation (MIMO-OFDM-IM), which provides a flexible trade-off between spectral efficiency and error performance, is recently proposed as a promising transmission technique for energy-efficient 5G wireless communication systems. However, due to the dependence of subcarrier symbols within each subblock and the strong inter-channel interference, it is challenging to detect the transmitted data effectively while imposing low computational burden to the receiver. In this paper, we propose a low-complexity detector based on the sequential Monte Carlo (SMC) theory for the detection of MIMO-OFDM-IM signals. The proposed detector, which draws samples based on the importance weights at the subblock level, achieves near-optimal error performance with considerably reduced computational complexity. Simulation and numerical results in terms of bit error rate (BER) and number of complex multiplications (NCM) corroborate the superiority of the proposed detector.**

I. Introduction

Recently, a novel MIMO scheme called spatial modulation (SM) has emerged as an appealing candidate to fulfill the spectral and energy efficiency requirements of the next generation wireless communication systems [1], [2]. In SM, information bits are conveyed not only by the modulated symbol, but also by the index of the active transmit antenna. By replacing the antenna indices in the MIMO system with the subcarrier indices of the orthogonal frequency division multiplexing (OFDM) signal, the concept of SM has been successfully transplanted to OFDM systems [3], [4]. As the representative frequency-domain extension of SM, OFDM with index modulation (OFDM-IM), which activates a subset of subcarriers to carry the modulated symbols simultaneously, is proposed in [4]. In OFDM-IM, the information is embedded in both subcarrier indices and M-ary constellation domains. Compared with classical OFDM, OFDM-IM provides a more flexible trade-off between the spectral efficiency and the error performance, and has the potential to achieve much better bit error rate performance for low-to-mid spectral efficiencies [4].

Owing to its interesting properties and superior BER performance, OFDM-IM has attracted considerable research interest over the past few years [5]–[11]. A subcarrier-level interleaving method is proposed for OFDM-IM to attain coding gains from uncorrelated subcarriers [5]. In [6], OFDM-IM coupled with the coordinate interleaving principle is proposed to explore potential diversity gains of OFDM-IM. By extending the index modulation to include both the in-phase and quadrature dimensions, a generalization of OFDM-IM is proposed with a low-complexity maximum-likelihood (ML) detector [7]. While the performance of OFDM-IM is analyzed in terms of ergodic achievable rate [8] and average mutual information [9].

More recently, by combining OFDM-IM with MIMO transmission techniques, a novel scheme called MIMO-OFDM-IM is presented in [10], which exhibits the potential to surpass the classical MIMO-OFDM. Then, the error performance of the MIMO-OFDM-IM scheme is investigated theoretically for different types of detectors in [11]. In this scheme, since each transmit antenna transmits an independent OFDM-IM block, its spectral efficiency can reach T times that of OFDM-IM, where T denotes the number of transmit antennas. However, due to the dependence of the subcarrier symbols within each OFDM-IM subblock and the strong inter-channel interference (ICI) between the transmit antennas of the MIMO-OFDM-IM system, it becomes much more challenging to detect the active subcarrier indices and modulated symbols. Although the ML detector is able to achieve optimal performance, it necessitates an exhaustive search with prohibitive computational complexity, which makes itself impractical for MIMO-OFDM-IM. To reduce the detection complexity, a log-likelihood ratio (LLR) based detector coupled with the minimum mean square error (MMSE) filter is then proposed for the detection of MIMO-OFDM-IM, which, however, suffers from a significant error performance loss compared to the ML detector. Therefore, the design of the low-complexity detector for MIMO-OFDM-IM with near-optimal error performance remains an open as well as challenging research problem.

In this paper, in order to achieve near-optimal error performance while maintaining low computational complexity, a novel detection algorithm based on the sequential Monte Carlo (SMC) theory is proposed for MIMO-OFDM-IM. By regarding each OFDM-IM subblock as a super modulated symbol drawn from a large finite set, the proposed detector draws samples independently at the subblock level to achieve near-optimal performance with substantially reduced complexity. Computer simulation and numerical results in terms of BER and NCM corroborate the superiority of our proposed detection method.

Notation: Upper and lower case boldface letters denote matrices and column vectors, respectively. $(\cdot)^{\mathrm{T}}$, $(\cdot)^{\mathrm{H}}$, and $(\cdot)^{-1}$

This work was supported in part by the National Natural Science Foundation of China (No. 61431005, 61501190, 61671211, 61501531), by the Natural Science Foundation of Guangdong Province (No. 2016A030311024), by the open research fund of National Mobile Communications Research Laboratory, Southeast University (No. 2017D08), and by the China Scholarship Council.

978-1-4673-8999-0/17/$31.00 ©2017 IEEE

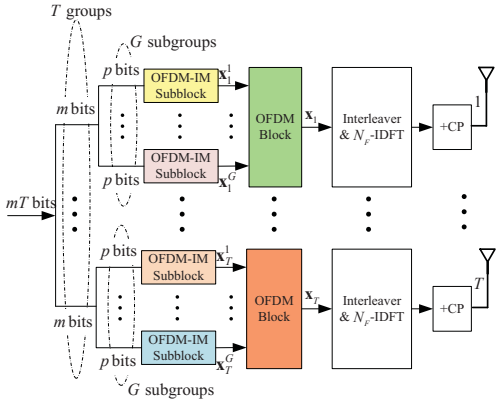

Fig. 1. Block diagram of MIMO-OFDM-IM transmitter.

stand for transpose, Hermitian transpose, and matrix inversion operations, respectively. $(\cdot)^{(b)}$ denotes the b-th particle drawn by the SMC sampling, its associated importance weight, or its prediction distribution. $(\cdot)_{[i]}$ denotes the hypothesis drawn with the sample being the i-th element of a finite set, its associated importance weight, or its prediction distribution. $\mathrm{diag}\{\mathbf{x}\}$ returns a diagonal matrix whose diagonal elements are included in $\mathbf{x}$. $|\cdot|$ denotes the absolute value if applied to a complex number or the cardinality if applied to a set. The probability density function (PDF) and the probability mass function (PMF) are denoted by $p(\cdot)$ and $P(\cdot)$, respectively. $\|\cdot\|_p$ denotes the ℓ_p-norm and $\emptyset$ represents the empty set. $\lfloor\cdot\rfloor$ denotes the floor function and $\mathrm{count}(\cdot)$ returns the number of non-zero elements in a set or a vector. $\binom{N}{K}$ denotes the binomial coefficient, which is defined to be zero if $N < K$.

II. Overview of MIMO-OFDM-IM

In this paper, we consider a MIMO-OFDM-IM system equipped with T transmit and R receive antennas [10], [11]. The block diagram of the MIMO-OFDM-IM transmitter is depicted in Fig. 1. Each MIMO-OFDM-IM frame is comprised of a total number of mT incoming data bits. These bits are divided into T groups, each of which contains m bits for the generation of an OFDM-IM block to be transmitted from a transmit antenna. These m bits are further divided into G subgroups, each of which consists of p bits, i.e., $m = Gp$. Assuming N_F available subcarriers of each block, each subgroup is then used to generate an OFDM-IM subblock consisting of $N = N_F/G$ subcarriers.

Unlike classical OFDM, which maps all data bits to the constellation points for all subcarriers, OFDM-IM separates p bits of each subblock into two parts for different purposes: the first part with $p_1 = \lfloor \log_2 \binom{N}{K} \rfloor$ bits is used to select K active subcarriers, while the remaining $N - K$ subcarriers are set to be idle;[1] the second part with $p_2 = K \log_2 M$ bits is mapped into K modulated symbols for the K active subcarriers via M-ary modulation. The mapping between the p_1 bits and the subcarrier combination patterns can be implemented by using a look-up table or the combinatorial method [4]. Consider the g-th ($1 \le g \le G$) OFDM-IM subblock at the t-th ($1 \le t \le T$) transmit antenna. Accordingly, the output of the first part is the indices of K active subcarriers, which are represented by the set $J_t^g = \{j_t^g(1), \ldots, j_t^g(K)\}$, where the elements of J_t^g are sorted in an ascending order, i.e., $1 \le j_t^g(1) < \cdots < j_t^g(K) \le N$. The output of the second part is K modulated symbols $\{s_t^g(n)\}_{n \in J_t^g}$, where $s_t^g(n)$ is drawn from a complex alphabet and the normalization of signal constellation is assumed. Therefore, the g-th OFDM-IM subblock element at the t-th transmit antenna can be expressed as $\mathbf{x}_t^g = [x_t^g(1)\ x_t^g(2)\ \cdots\ x_t^g(N)]^{\mathrm{T}}$, where

$$x_t^g(n) = \begin{cases} s_t^g(n), & n \in J_t^g \\ 0, & \text{otherwise} \end{cases}. \tag{1}$$

After generating all OFDM-IM subblocks, each OFDM-IM block is created by concatenating G OFDM-IM subblocks in each branch of the transmitter, which is denoted by $\mathbf{x}_t = \left[\left(\mathbf{x}_t^1\right)^{\mathrm{T}}\ \left(\mathbf{x}_t^2\right)^{\mathrm{T}}\ \cdots\ \left(\mathbf{x}_t^G\right)^{\mathrm{T}}\right]^{\mathrm{T}} \triangleq [x_t(1)\ x_t(2)\ \cdots\ x_t(N_F)]^{\mathrm{T}}$, where $1 \le t \le T$. To fully benefit from the frequency-selective fading, a $G \times N$ block interleaver is employed in each branch of the transmitter. Before transmission, each OFDM-IM block is first transformed into the time-domain signal block by employing an N_F-point inverse discrete Fourier transform (IDFT), and then appended with a CP longer than the maximum delay spread of the channel.

After passing through the frequency-selective MIMO channel, the CP is removed and an N_F-point discrete Fourier transform (DFT) followed by a $G \times N$ block deinterleaver is employed at each receive antenna to obtain the received block in the frequency domain. Specifically, for the r-th ($1 \le r \le R$) receive antenna, the g-th ($1 \le g \le G$) received subblock after block deinterleaving can be expressed as

$$\mathbf{y}_r^g = \sqrt{\frac{\rho}{T}} \sqrt{\frac{N}{K}} \sum_{t=1}^{T} \mathrm{diag}\left\{\mathbf{h}_{r,t}^g\right\} \mathbf{x}_t^g + \mathbf{w}_r^g \tag{2}$$

where $\mathbf{y}_r^g \triangleq [y_r^g(1)\ y_r^g(2)\ \cdots\ y_r^g(N)]^{\mathrm{T}}$, ρ is signal-to-noise ratio (SNR) per receive antenna, $\mathbf{h}_{r,t}^g$ denotes the corresponding channel vector of dimensions $N \times 1$ which contains the channel frequency responses (CFRs) for the g-th OFDM-IM subblock, and $\mathbf{w}_r^g \sim \mathcal{N}_c(0, \mathbf{I}_N)$ is the additive white Gaussian noise (AWGN) vector. Furthermore, for the n-th ($1 \le n \le N$) subcarrier of the g-th ($1 \le g \le G$) OFDM-IM subblock, the signal vector observed at the receiver can be collected as

$$\underbrace{\begin{bmatrix} y_1^g(n) \\ y_2^g(n) \\ \vdots \\ y_R^g(n) \end{bmatrix}}_{\bar{\mathbf{y}}_n^g} = \sqrt{\frac{\rho}{T}} \sqrt{\frac{N}{K}} \underbrace{\begin{bmatrix} h_{1,1}^g(n) & h_{1,2}^g(n) & \ldots & h_{1,T}^g(n) \\ h_{2,1}^g(n) & h_{2,2}^g(n) & \ldots & h_{2,T}^g(n) \\ \vdots & \vdots & \ddots & \vdots \\ h_{R,1}^g(n) & h_{R,2}^g(n) & \ldots & h_{R,T}^g(n) \end{bmatrix}}_{\bar{\mathbf{H}}_n^g} \times \underbrace{\begin{bmatrix} x_1^g(n) \\ x_2^g(n) \\ \vdots \\ x_T^g(n) \end{bmatrix}}_{\bar{\mathbf{x}}_n^g} + \underbrace{\begin{bmatrix} w_1^g(n) \\ w_2^g(n) \\ \vdots \\ w_R^g(n) \end{bmatrix}}_{\bar{\mathbf{w}}_n^g} \tag{3}$$

[1] Note that to modulate an integer number of bits, only $N_C = 2^{p_1}$ subcarrier combination patterns are permitted and the remaining $\binom{N}{K} - N_C$ patterns are considered to be illegal.

where $\bar{\mathbf{y}}_n^g$ is the received signal vector, $\bar{\mathbf{H}}_n^g$ is the corresponding channel matrix which contains the CFRs between the transmit and receive antennas, $\bar{\mathbf{x}}_n^g$ is the data vector which contains the simultaneously transmitted symbols from all transmit antennas, and $\bar{\mathbf{w}}_n^g \sim \mathcal{N}_c(0, \mathbf{I}_R)$ is an $R \times 1$ AWGN vector whose elements have zero mean and unit variance. After applying the matched filter and noise whitening to (3), the output can be written as

$$\tilde{\mathbf{y}}_n^g \triangleq (\mathbf{A}_n^g)^{-1/2} \left(\bar{\mathbf{H}}_n^g\right)^{\mathrm{H}} \bar{\mathbf{y}}_n^g = \sqrt{\frac{\rho}{T}}\sqrt{\frac{N}{K}} (\mathbf{A}_n^g)^{1/2} \bar{\mathbf{x}}_n^g + \tilde{\mathbf{w}}_n^g \quad (4)$$

where $\mathbf{A}_n^g = \left(\bar{\mathbf{H}}_n^g\right)^{\mathrm{H}} \bar{\mathbf{H}}_n^g$, and $\tilde{\mathbf{w}}_n^g = (\mathbf{A}_n^g)^{-1/2} \left(\bar{\mathbf{H}}_n^g\right)^{\mathrm{H}} \bar{\mathbf{w}}_n^g$ is a $T \times 1$ AWGN vector whose elements have zero-mean and unit variance. Let us stack the received signal vectors in (4) for N consecutive subcarriers of the g-th ($1 \le g \le G$) OFDM-IM subblock, which can be expressed as

$$\underbrace{\begin{bmatrix} \tilde{\mathbf{y}}_1^g \\ \tilde{\mathbf{y}}_2^g \\ \vdots \\ \tilde{\mathbf{y}}_N^g \end{bmatrix}}_{\tilde{\mathbf{y}}^g} = \sqrt{\frac{\rho}{T}}\sqrt{\frac{N}{K}} \underbrace{\begin{bmatrix} (\mathbf{A}_1^g)^{1/2} & \mathbf{0} & \dots & \mathbf{0} \\ \mathbf{0} & (\mathbf{A}_2^g)^{1/2} & \dots & \mathbf{0} \\ \vdots & \vdots & \ddots & \vdots \\ \mathbf{0} & \mathbf{0} & \dots & (\mathbf{A}_N^g)^{1/2} \end{bmatrix}}_{\tilde{\mathbf{A}}^g} \times \underbrace{\begin{bmatrix} \bar{\mathbf{x}}_1^g \\ \bar{\mathbf{x}}_2^g \\ \vdots \\ \bar{\mathbf{x}}_N^g \end{bmatrix}}_{\tilde{\mathbf{x}}^g} + \underbrace{\begin{bmatrix} \tilde{\mathbf{w}}_1^g \\ \tilde{\mathbf{w}}_2^g \\ \vdots \\ \tilde{\mathbf{w}}_N^g \end{bmatrix}}_{\tilde{\mathbf{w}}_n^g} \quad (5)$$

where $\tilde{\mathbf{y}}^g$ is the received signal vector after stacking, $\tilde{\mathbf{A}}^g$ is a block diagonal channel matrix whose diagonal elements are $(\mathbf{A}_n^g)^{1/2}$ with $n = 1, \dots, N$ and the off-diagonal elements are zero matrices $\mathbf{0}$ of size $T \times T$, $\tilde{\mathbf{x}}^g$ is the data vector after stacking all g-th OFDM-IM subblocks, and $\tilde{\mathbf{w}}^g$ is a $TN \times 1$ zero-mean AWGN vector with unit variance elements.

By considering a joint detection for all g-th OFDM-IM subblocks from different transmit antennas, the ML detector based on (5) for MIMO-OFDM-IM is given by

$$\hat{\tilde{\mathbf{x}}}^g = \arg\min_{\tilde{\mathbf{x}}^g} \left\| \tilde{\mathbf{y}}_n^g - \sqrt{\frac{\rho}{T}}\sqrt{\frac{N}{K}} \tilde{\mathbf{A}}^g \tilde{\mathbf{x}}^g \right\|^2. \quad (6)$$

Although the ML detector can achieve optimal error performance, its computational complexity increases exponentially with the number of transmit antennas. From (6), it can be observed that the search complexity per subblock is of order $\left(N_C M^K\right)^T$ for the ML detector, which is costly and even infeasible for the practical implementation of the receiver.

III. Low-Complexity Detector Design

In this section, we will develop a novel detector for MIMO-OFDM-IM based on deterministic SMC, whose objective is to approximate the *a posteriori* distributions of the states of some Markov processes, given some noisy and partial observations [12]. As will be shown by simulations, the proposed detector can save computational complexity significantly and provide near-optimal performance for MIMO-OFDM-IM.

A. Sequential Structure for MIMO-OFDM-IM

To apply the SMC theory to the detection of MIMO-OFDM-IM, we first construct the sequential structure based on the observed signals. Inspired by the successive interference cancellation (SIC) method for the MIMO detection [13], we apply the QL decomposition[2] to the matrix $(\mathbf{A}_n^g)^{1/2}$ in (4) as

$$(\mathbf{A}_n^g)^{1/2} = \mathbf{Q}_n^g \mathbf{L}_n^g, \qquad n = 1, \dots, N,\ g = 1, \dots, G \quad (7)$$

where $\mathbf{Q}_n^g$ is a unitary matrix, and $\mathbf{L}_n^g$ is a lower triangular matrix. The lower triangular operation is carried out by the left multiplication of the vector $\tilde{\mathbf{y}}_n^g$ in (4) by $(\mathbf{Q}_n^g)^{\mathrm{H}}$ to obtain $\bar{\mathbf{z}}_n^g = (\mathbf{Q}_n^g)^{\mathrm{H}} \tilde{\mathbf{y}}_n^g$, which can be further written as

$$\underbrace{\begin{bmatrix} z_1^g(n) \\ z_2^g(n) \\ \vdots \\ z_T^g(n) \end{bmatrix}}_{\bar{\mathbf{z}}_n^g} = \sqrt{\frac{\rho}{T}}\sqrt{\frac{N}{K}} \underbrace{\begin{bmatrix} l_{1,1}^g(n) & & & \\ l_{2,1}^g(n) & l_{2,2}^g(n) & & \\ \vdots & \vdots & \ddots & \\ l_{T,1}^g(n) & l_{T,2}^g(n) & \dots & l_{T,T}^g(n) \end{bmatrix}}_{\mathbf{L}_n^g} \times \underbrace{\begin{bmatrix} x_1^g(n) \\ x_2^g(n) \\ \vdots \\ x_T^g(n) \end{bmatrix}}_{\bar{\mathbf{x}}_n^g} + \underbrace{\begin{bmatrix} v_1^g(n) \\ v_2^g(n) \\ \vdots \\ v_T^g(n) \end{bmatrix}}_{\bar{\mathbf{v}}_n^g} \quad (8)$$

where $\bar{\mathbf{v}}_n^g = (\mathbf{Q}_n^g)^{\mathrm{H}} \tilde{\mathbf{w}}_n^g$ is still a $T \times 1$ zero-mean AWGN vector with unit variance elements as the matrix $\mathbf{Q}_n^g$ is unitary. Based on the structure in (8), the SIC may be applied to detect the data vector $\bar{\mathbf{x}}_n^g$ in a sequential manner, i.e., the interference due to the previously decoded subblocks is subtracted from the observed sample before decoding the next subblock. However, as the SIC method is known to suffer from the error propagation problem, we will not employ the SIC method but instead exploit the aforementioned sequential structure for the low-complexity detector design of MIMO-OFDM-IM.

B. Deterministic SMC Aided Subblock-wise Detection

After the lower triangular operation, the sequential structure in (8) can be exploited by applying the SMC method to draw samples starting from the first transmit antenna and ending to the last one. Indeed, if we simply regard each OFDM-IM subblock $\mathbf{x}_t^g$ as a super modulated symbol drawn from a large finite set, we have the *a posteriori* distribution of $\{\mathbf{x}_t^g\}_{t=1}^T$ conditioned on $\{\mathbf{z}_t^g\}_{t=1}^T$ as

$$P\left(\{\mathbf{x}_t^g\}_{t=1}^T \middle| \{\mathbf{z}_t^g\}_{t=1}^T\right) \propto \prod_{t=1}^T p\left(\mathbf{z}_t^g \middle| X_t^g\right) P\left(\mathbf{x}_t^g\right) \quad (9)$$

where $\mathbf{z}_t^g \triangleq [z_t^g(1)\ z_t^g(2)\ \cdots\ z_t^g(N)]^{\mathrm{T}}$ denotes the observed subblock in the t-th ($1 \le t \le T$) branch of the receiver after the lower triangular operation in (8), and $X_t^g \triangleq \{\mathbf{x}_{t'}^g\}_{t'=1}^t$. Based on (9), we turn to construct the sequence of probability distributions $\left\{P\left(X_t^g \middle| Z_t^g\right)\right\}_{t=1}^T$, where $Z_t^g \triangleq \{\mathbf{z}_{t'}^g\}_{t'=1}^t$. Specifically, the sequential distributions can be expressed as

[2]The QL decomposition can be obtained in analogy with the QR decomposition, which can be derived by using the Gram-Schmidt process starting from the last column of the designated matrix.

$$P\left(X_t^g\middle|Z_t^g\right)\propto\prod_{t'=1}^{t}p\left(\mathbf{z}_{t'}^g\middle|X_{t'}^g\right)P\left(\mathbf{x}_{t'}^g\right)\tag{10}$$

for $t=1,\ldots,T$. From the perspective of the probability theory, our aim is to estimate the *a posteriori* probability of each OFDM-IM subblock

$$P\left(\mathbf{x}_t^g=\mathbf{\Phi}_i\middle|\left\{\mathbf{z}_t^g\right\}_{t=1}^T\right),\quad\mathbf{\Phi}_i\in\tilde{\mathbf{\Phi}},\ t=1,\ldots,T\tag{11}$$

based on the observed subblocks $\{\mathbf{z}_t^g\}_{t=1}^T$, where $\tilde{\mathbf{\Phi}}\triangleq\{\mathbf{\Phi}_i\}_{i=1}^{N_CM^K}$ with $|\tilde{\mathbf{\Phi}}|=N_CM^K$ denotes the set including all possible realizations of the OFDM-IM subblock. Instead of the direct computation of (11), which is too computationally expensive, we seek to numerically approximate (11) by using the deterministic SMC theory to substantially reduce the complexity at the receiver.

Let $\left(X_t^g\right)^{(b)}$ with $b=1,\ldots,\beta$ be the particles drawn by the SMC method at each sampling interval on the basis of subblock, where β denotes the total number of particles. To implement the SMC method, we first need to generate a set of incomplete particles for the OFDM-IM subblocks, and then update the corresponding importance weights for those particles with respect to the distribution of (9) until the subblock at the last antenna is reached. Moreover, to update the importance weights, it is crucial to design the trial distribution which minimizes the variance of the importance weights conditioned upon the previous particles and the observed signals [12]. Under the criterion of minimum conditional variance of the importance weights, we simply choose the trial distribution as

$$\psi\left(\mathbf{x}_t^g\middle|Z_t^g,\left(X_{t-1}^g\right)^{(b)}\right)\propto P\left(\mathbf{x}_t^g\middle|Z_t^g,\left(X_{t-1}^g\right)^{(b)}\right)\tag{12}$$

for $t=1,\ldots,T$.

Proposition 1: With the trial distribution given in (12), the importance weight for the SMC can be updated according to

$$\left(\varpi_t^g\right)^{(b)}\propto\left(\varpi_{t-1}^g\right)^{(b)}\cdot p\left(\mathbf{z}_t^g\middle|\left(X_{t-1}^g\right)^{(b)}\right)\tag{13}$$

where $p\left(\mathbf{z}_t^g\middle|\left(X_{t-1}^g\right)^{(b)}\right)$ can be regarded as the prediction distribution of the current observed subblock $\mathbf{z}_t^g$ under the condition of the previous particle $\left(X_{t-1}^g\right)^{(b)}$.

Proof: See Appendix. ■

In MIMO-OFDM-IM, each OFDM-IM subblock has a finite number of realizations, i.e., N_CM^K. For this reason, the deterministic SMC sampling can be applied by first enumerating all possible subblock realizations at each sampling interval and then calculating their associated prediction distributions exactly based on the previous particles paired with the specific subblock sample. In other words, with the given particle $\left(X_{t-1}^g\right)^{(b)}$, we can calculate each prediction distribution

$$\left(\gamma_t^g\right)_{[i]}^{(b)}\triangleq p\left(\mathbf{z}_t^g\middle|\mathbf{x}_t^g=\mathbf{\Phi}_i,\left(X_{t-1}^g\right)^{(b)}\right)\tag{14}$$

for $\mathbf{\Phi}_i\in\tilde{\mathbf{\Phi}}$ to get a more precise result. If the specific subblock sample $\mathbf{x}_t^g=\mathbf{\Phi}_i$ is assumed in the prediction distribution, the update for the importance weight in (13) can be revised as

$$\left(\varpi_t^g\right)_{[i]}^{(b)}\propto\left(\varpi_{t-1}^g\right)^{(b)}\cdot\left(\gamma_t^g\right)_{[i]}^{(b)}\cdot P\left(\mathbf{x}_t^g=\mathbf{\Phi}_i\right)\tag{15}$$

$$\propto\left(\varpi_{t-1}^g\right)^{(b)}\cdot\left(\gamma_t^g\right)_{[i]}^{(b)}\tag{16}$$

where $i=1,\ldots,N_CM^K$, and (16) holds due to the equal probability assumption for all subblock realizations. Since the noise vector $\bar{\mathbf{v}}_n^g=\left(\mathbf{Q}_n^g\right)^{\mathrm{H}}\tilde{\mathbf{w}}_n^g$ in (8) is white Gaussian, the prediction distribution $\left(\gamma_t^g\right)_{[i]}^{(b)}$ can be expressed as

$$\left(\gamma_t^g\right)_{[i]}^{(b)}=\frac{1}{\pi^N}\exp\left\{-\left\|\mathbf{z}_t^g-\left(\mathbf{u}_t^g\right)_{[i]}^{(b)}\right\|^2\right\}\tag{17}$$

where $\left(\mathbf{u}_t^g\right)_{[i]}^{(b)}\triangleq\left[\left(u_t^g(1)\right)_{[i]}^{(b)}\ \left(u_t^g(2)\right)_{[i]}^{(b)}\ \cdots\ \left(u_t^g(N)\right)_{[i]}^{(b)}\right]^{\mathrm{T}}$ denotes the mean vector of $\mathbf{z}_t^g$, whose n-th ($1\le n\le N$) element is given by

$$\begin{aligned}\left(u_t^g(n)\right)_{[i]}^{(b)}=&\sqrt{\frac{\rho}{T}}\sqrt{\frac{N}{K}}\sum_{t'=1}^{t-1}l_{t,t'}^g(n)\left(x_{t'}^g(n)\right)^{(b)}\\&+\sqrt{\frac{\rho}{T}}\sqrt{\frac{N}{K}}l_{t,t}^g(n)\Phi_i(n)\end{aligned}\tag{18}$$

with $\Phi_i(n)$ being the n-th element of the sample vector $\mathbf{\Phi}_i$.

With the update of the importance weights in (16), we further need to determine the initial particles and their corresponding importance weights. In the initialization of the deterministic SMC, we will compute the *a posteriori* distributions $P\left(X_\Gamma^g\middle|Z_\Gamma^g\right)$ exactly by enumerating all possible realizations of X_Γ^g corresponding to the g-th subblocks from the first transmit antenna to the Γ-th one, where the total number of all possible realizations is $|\tilde{\mathbf{\Phi}}|^\Gamma$ and $\Gamma<T$.[3] According to the deterministic SMC and (8), the *a posteriori* probabilities $P\left(\left(X_\Gamma^g\right)^{(b)}\middle|Z_\Gamma^g\right)$, which act as the initial importance weights of particles $\left(X_\Gamma^g\right)^{(b)}$, can be expressed as

$$\left(\varpi_\Gamma^g\right)^{(b)}=P\left(\left(X_\Gamma^g\right)^{(b)}\middle|Z_\Gamma^g\right)\propto\prod_{t=1}^{\Gamma}\left(\gamma_t^g\right)_{[i]}^{(b)}.\tag{19}$$

where $b=1,\ldots,\beta$ and $\left\{\left(X_\Gamma^g\right)^{(b)}\right\}_{b=1}^{\beta}$ contains all possible realizations of X_Γ^g if $\beta=|\tilde{\mathbf{\Phi}}|^\Gamma$. After the initialization, the importance weights are updated according to (16). At each sampling interval on the basis of subblock, current β particles with the highest importance weights are selected as the survivors over $\beta|\tilde{\mathbf{\Phi}}|$ possible hypotheses departed from the previous particles. When the recursion reaches the last sampling interval, i.e., $t=T$, β particles and the corresponding importance weights are then used to estimate the *a posteriori* probability for each subblock in (11), given by

$$P\left(\mathbf{x}_t^g=\mathbf{\Phi}_i\middle|\left\{\mathbf{z}_t^g\right\}_{t=1}^T\right)\cong\frac{1}{\widetilde{\varpi}_T^g}\sum_{b=1}^{\beta}I\left(\left(\mathbf{x}_t^g\right)^{(b)};\mathbf{\Phi}_i\right)\left(\varpi_T^g\right)^{(b)}\tag{20}$$

where $\mathbf{\Phi}_i\in\tilde{\mathbf{\Phi}}$, $\widetilde{\varpi}_T^g=\sum_{b=1}^{\beta}\left(\varpi_T^g\right)^{(b)}$, and $I(;)$ denotes the indicator function [14]. Notably, the importance weights obtained at the last sampling interval is applied to compute the *a posteriori* subblock probabilities, for those weights provide better estimations [15] and we detect the corresponding subblocks at the last step. Moreover, the *a posteriori* probability

[3] If $\Gamma\ge T$, we can compute $P\left(X_T^g\middle|Z_T^g\right)$ exactly based on the deterministic SMC; however, it is too computationally expensive.

Algorithm 1 Deterministic SMC aided subblock-wise detection

1: Perform the lower triangular operation to obtain (8) and initiate the particles coupled with the importance weights via (19);
2: **for** $t = \Gamma + 1$ to T **do**
3: Update the importance weights according to (16), $b = 1, \ldots, \beta$;
4: Pick up and retain β particles with the highest importance weights among the $\beta|\tilde{\mathbf{\Phi}}|$ hypotheses with weights set $\left\{(\varpi_t^g)_{[i]}^{(b)}\right\}$, $b = 1, \ldots, \beta$, $i = 1, \ldots, N_C M^K$;
5: **end for**
6: Compute the *a posteriori* probability for each subblock via (20), and the estimate of each subblock is given by $\widehat{\mathbf{x}}_t^g = \arg\max_{\mathbf{\Phi}_i \in \tilde{\mathbf{\Phi}}} P\left(\mathbf{x}_t^g = \mathbf{\Phi}_i \middle| \{\mathbf{z}_t^g\}_{t=1}^T\right)$, $t = 1, \ldots, T$.

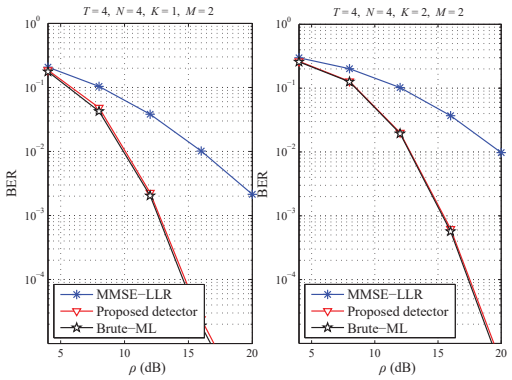

Fig. 2. BER performance comparison of different detection algorithms for MIMO-OFDM-IM with $T = 4$, $N = 4$, and BPSK modulation.

estimated in (20) can be readily applied to the detection with soft output, which is compatible with the coded system. Finally, we summarize the deterministic SMC aided subblock-wise detection in Algorithm 1.

IV. Simulation and Numerical Results

In this section, we verify the effectiveness of the proposed detection algorithm for MIMO-OFDM-IM via computer simulation and numerical results. In the simulations, a MIMO channel with frequency-selective Rayleigh fading is considered, where the maximum delay spread of the channel is equal to $10 \times T_s$, where T_s denotes the sampling period of the digital system. Each OFDM-IM block consists of $N_F = 512$ subcarriers and is appended by a CP of length 16. It is assumed that channel state information is unknown to the transmitter but perfectly estimated at the receiver. For ease of comparison, the number of receive antennas is set to be equal to the number of transmit antennas, i.e., $R = T$, and the number of particles drawn by the proposed detector is set to be $\beta = 8$.

A. Error Performance Comparison

Fig. 2 shows the BER comparison results of different detection algorithms for the MIMO-OFDM-IM system with $T = 4$, $N = 4$, and BPSK modulation. It can be observed that the proposed subblock-wise detector achieves near-optimal performance while the MMSE-LLR detector suffers from a significant performance loss. By comparing the two scenarios with different number of active subcarriers ($K = 1$ and $K = 2$), we observe that the BER performance of all detectors degrades as the number of active subcarriers increases. This can be understood as each active subcarrier will be allocated less power when more subcarriers are activated for transmission.

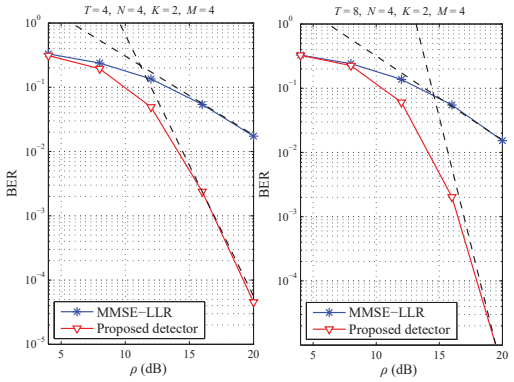

Fig. 3. BER performance comparison of different detection algorithms for MIMO-OFDM-IM with $N = 4$, $K = 2$, and QPSK modulation.

In Fig. 3, the BER performance of different detection algorithms is compared for the MIMO-OFDM-IM system with $N = 4$, $K = 2$, and QPSK modulation. As the ML detection requires an immense amount of computation, its BER curve is not shown in Fig. 3. It can be seen that the proposed detector outperforms the MMSE-LLR detector significantly. Moreover, we observe that unlike the MMSE-LLR detector, the BER performance of the proposed detector is improved as the number of receive antennas ($R = T$) increases. This can be understood since the diversity order of the MMSE-LLR detector is equal to one regardless of the number of receive antennas while a diversity order of R is obtained by the proposed detector.

B. Complexity Comparison

In Fig. 4, the computational complexity for different types of detectors is compared in terms of exact NCM performed per subcarrier. As expected, the computational complexity of the ML detection is prohibitive and increases exponentially with the number of transmit antennas. However, our proposed detectors achieves rather low computational complexity, which is comparable to that of the MMSE-LLR detector. Interestingly, the computational complexity of the MMSE-LLR detector seems to be more susceptible to the number of transmit antennas and the proposed detector has the potential to achieve lower complexity than the MMSE-LLR detector when the number of transmit antennas becomes large. In summary, the proposed detection algorithms achieve near-optimal performance while maintaining considerably lower complexity that is comparable to that of the MMSE-LLR detector.

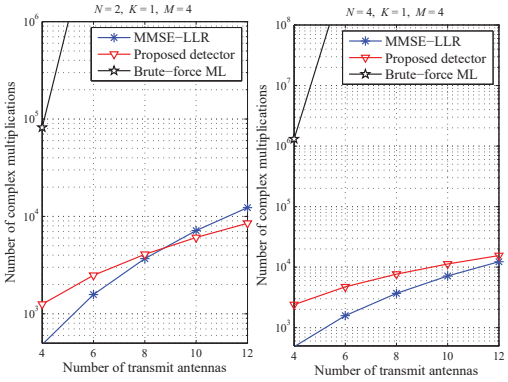

Fig. 4. Complexity comparison of different detection algorithms for MIMO-OFDM-IM with $K = 1$, and QPSK modulation.

V. Conclusion

In this paper, we have proposed a novel low-complexity detectors derived from the SMC theory for the MIMO-OFDM-IM system. The proposed detector draws samples at the subblock level, exhibiting near-optimal performance for the MIMO-OFDM-IM system. Computer simulation and numerical results have validated the outstanding performance and the low complexity of the proposed detector. In the future, we would like to design another SMC based detector that draws samples at the subcarrier level to further reduce the computational complexity and investigate the performance analysis.

Appendix
Proof of Proposition 1

According to [12] and [16], the importance weight is given by

$$\left(\varpi_t^g\right)^{(b)} = \frac{P\left(\left(X_t^g\right)^{(b)} \middle| Z_t^g\right)}{\psi\left(\left(X_t^g\right)^{(b)} \middle| Z_t^g\right)}. \tag{21}$$

Although (21) is not sequential, we can come up with a sequential version by exploiting the property of the trial distribution. In order to work in a sequential manner, the trial distribution is supposed to satisfy

$$\psi\left(X_t^g \middle| Z_t^g\right) = \psi\left(X_1^g \middle| Z_1^g\right) \prod_{t'=2}^{t} \psi\left(\mathbf{x}_{t'}^g \middle| X_{t'-1}^g, Z_{t'}^g\right). \tag{22}$$

Furthermore, (22) can be rewritten in a recursive form as

$$\psi\left(X_t^g \middle| Z_t^g\right) = \psi\left(X_{t-1}^g \middle| Z_{t-1}^g\right) \psi\left(\mathbf{x}_t^g \middle| X_{t-1}^g, Z_t^g\right). \tag{23}$$

Based on (21) and (23), the update recursions for the importance weights are then given by

$$\left(\varpi_t^g\right)^{(b)} = \left(\varpi_{t-1}^g\right)^{(b)} \times \frac{P\left(\left(X_t^g\right)^{(b)} \middle| Z_t^g\right)}{\psi\left(\left(X_{t-1}^g\right)^{(b)} \middle| Z_{t-1}^g\right) \psi\left(\left(\mathbf{x}_t^g\right)^{(b)} \middle| \left(X_{t-1}^g\right)^{(b)}, Z_t^g\right)} \tag{24}$$

where $b = 1, \ldots, \beta$. With the trial distribution of (12) satisfying (23), (24) can be further written as

$$\left(\varpi_t^g\right)^{(b)} \propto \left(\varpi_{t-1}^g\right)^{(b)} \times \frac{P\left(\left(X_t^g\right)^{(b)} \middle| Z_t^g\right)}{P\left(\left(X_{t-1}^g\right)^{(b)} \middle| Z_{t-1}^g\right) P\left(\left(\mathbf{x}_t^g\right)^{(b)} \middle| \left(X_{t-1}^g\right)^{(b)}, Z_t^g\right)} \tag{25}$$

$$= \left(\varpi_{t-1}^g\right)^{(b)} \cdot \frac{P\left(\left(X_{t-1}^g\right)^{(b)} \middle| Z_t^g\right)}{P\left(\left(X_{t-1}^g\right)^{(b)} \middle| Z_{t-1}^g\right)} \tag{26}$$

$$\propto \left(\varpi_{t-1}^g\right)^{(b)} \cdot p\left(\mathbf{z}_t^g \middle| Z_{t-1}^g, \left(X_{t-1}^g\right)^{(b)}\right) \tag{27}$$

$$= \left(\varpi_{t-1}^g\right)^{(b)} \cdot p\left(\mathbf{z}_t^g \middle| \left(X_{t-1}^g\right)^{(b)}\right) \tag{28}$$

where (26) holds due to the independence of the previous particle $\left(X_{t-1}^g\right)^{(b)}$ and the current subblock $\mathbf{x}_t^g$, (27) is obtained by neglecting the constant term $p\left(Z_{t-1}^g\right)/p\left(Z_t^g\right)$, and (28) holds due to the independence of the noise samples, completing the proof.

References

[1] R. Y. Mesleh, H. Haas, S. Sinanovic, C. W. Ahn, and S. Yun, "Spatial modulation," *IEEE Trans. Veh. Technol.*, vol. 57, no. 4, pp. 2228–2241, Jul. 2008.

[2] E. Basar, "Index modulation techniques for 5G wireless networks," *IEEE Commun. Mag.*, vol. 54, no. 7, pp. 168–175, Jul. 2016.

[3] R. Abu-alhiga and H. Haas, "Subcarrier-index modulation OFDM," in *Proc. IEEE PIMRC*, Tokyo, Japan, Sep. 2009, pp. 177–181.

[4] E. Basar, U. Aygolu, E. Panayirci, and H. V. Poor, "Orthogonal frequency division multiplexing with index modulation," *IEEE Trans. Signal Process.*, vol. 61, no. 22, pp. 5536–5549, Nov. 2013.

[5] Y. Xiao, S. Wang, L. Dan, X. Lei, P. Yang, and W. Xiang, "OFDM with interleaved subcarrier-index modulation," *IEEE Commun. Lett.*, vol. 18, no. 8, pp. 1447–1450, Aug. 2014.

[6] E. Basar, "OFDM with index modulation using coordinate interleaving," *IEEE Wireless Commun. Lett.*, vol. 4, no. 4, pp. 381–384, Aug. 2015.

[7] B. Zheng, F. Chen, M. Wen, F. Ji, H. Yu, and Y. Liu, "Low-complexity ML detector and performance analysis for OFDM with in-phase/quadrature index modulation," *IEEE Commun. Lett.*, vol. 19, no. 11, pp. 1893–1896, Nov. 2015.

[8] M. Wen, X. Cheng, M. Ma, B. Jiao, and H. V. Poor, "On the achievable rate of OFDM with index modulation," *IEEE Trans. Signal Process.*, vol. 64, no. 8, pp. 1919–1932, Apr. 2016.

[9] N. Ishikawa, S. Sugiura, and L. Hanzo, "Subcarrier-index modulation aided OFDM - will it work?" *IEEE Access*, vol. 4, pp. 2580–2593, Jun. 2016.

[10] E. Basar, "Multiple-input multiple-output OFDM with index modulation," *IEEE Signal Process. Lett.*, vol. 22, no. 12, pp. 2259–2263, Dec. 2015.

[11] ——, "On multiple-input multiple-output OFDM with index modulation for next generation wireless networks," *IEEE Trans. Signal Process.*, vol. 64, no. 15, pp. 3868–3878, Aug. 2016.

[12] A. Doucet, S. Godsill, and C. Andrieu, "On sequential Monte Carlo sampling methods for Bayesian filtering," *Statistics and computing*, vol. 10, no. 3, pp. 197–208, 2000.

[13] J.-K. Zhang, A. Kavcic, and K. M. Wong, "Equal-diagonal QR decomposition and its application to precoder design for successive-cancellation detection," *IEEE Trans. Inf. Theory*, vol. 51, no. 1, pp. 154–172, Jan. 2005.

[14] P. Aggarwal and X. Wang, "Multilevel sequential Monte Carlo algorithms for MIMO demodulation," *IEEE Trans. Wireless Commun.*, vol. 6, no. 2, pp. 750–758, Feb. 2007.

[15] R. Chen, X. Wang, and J. S. Liu, "Adaptive joint detection and decoding in flat-fading channels via mixture Kalman filtering," *IEEE Trans. Inf. Theory*, vol. 46, no. 6, pp. 2079–2094, Sep. 2000.

[16] B. Dong, X. Wang, and A. Doucet, "A new class of soft MIMO demodulation algorithms," *IEEE Trans. Signal Process.*, vol. 51, no. 11, pp. 2752–2763, Nov. 2003.